Journal of Engineering and Technology for Industrial Applications

ITEGAM-JETIA

Manaus, v.11 n.51, p. 43-55. January/February., 2025.
DOI: https://doi.org/10.5935/jetia.v11i51.1402

ISSN ONLINE: 2447-0228

RESEARCH ARTICLE OPEN ACCESS

A THREE PHASE INDUCTION MOTOR DYNAMIC FRAMEWORK REGULATED BY PREDICTIVE AND INTELLIGENT OPTIMIZATIONS

Shaswat Chirantan[1] and Bibhuti Bhusan Pati[2]

[1] PhD. Scholar, Department of Electrical Engineering, Veer Surendra Sai University of Technology, Burla, Sambalpur, 768018, India.
[2] Professor, Department of Electrical Engineering, Veer Surendra Sai University of Technology, Burla, Sambalpur, 768018, India.

[1]http://orcid.org/0000-0001-9052-3582, [2]http://orcid.org/0009-0009-3897-5712,

Email: shaswat.chirantan443@gmail.com, bbpati_ee@vssut.ac.in

ARTICLE INFO

Article History
Received: November 17, 2024
Revised: December 20, 2024
Accepted: January 15, 2025
Published: January 30, 2025

Keywords:
Model Predictive Control,
Predictive Current Control,
Finite Control Set,
Integral Finite Control Set,
Induction Motor,
Gravitational Search Algorithm ,
Genetic Algorithm.

ABSTRACT

The role of Model Predictive Control (MPC) as a fundamental optimization tool in modern control systems is increasingly emphasized. In this context, the paper presents Predictive Current Control (PCC) strategies for a three-phase inverter-fed induction motor drive (IM), focusing on two core approaches: the Finite Control Set (FCS) and the Integral Finite Control Set (IFCS). The FCS-MPC algorithm is based on the evaluation of a cost function, selecting a control signal from a finite set that satisfies the minimum value of the cost function. This cost function is calculated based on the squared error between the reference current and the measured stator current. Conversely, the I-FCS-MPC uses a cascade feedback structure with an appropriately adjusted controller gain to determine the optimal set of control variables. Using a minimization principle, these methods manage the switching states for reversal, causing the inverter to generate appropriate voltage signals for the induction motor. This article compares IM electromagnetic torque and load currents under each control technique to determine the most flexible and robust prediction strategy. All these methods were studied in the MATLAB/Simulink environment. In addition, the paper uses Gravitational Search Algorithm (GSA) and Genetic Algorithm (GA) as benchmarks and shows that the results of FCS and I-FCS methods have superior performance.

I. INTRODUCTION

In electrical engineering applications, MPC has proven to be more effective for utilizing and controlling the switching of power converters, synchronous and induction machine drives, as well as for controlling various power system parameters. Many researchers have implemented a wide range of predictive control algorithms. MPC has attracted wide attention due to its flexibility, robustness and fast dynamic response. The MPC topology can switch to two modes, i.e., depending on its operation and control actions and named as continuous control set (CCS), and finite control set (FCS). Predictive current control schemes for power converters and electric drives were proposed in [1], which demonstrates the CCS-MPC algorithm, the principle of receding horizon control with forward Euler approximation and cost function for a discrete-time load model of PMSM (permanent magnet synchronous motor) for switching states selection of the inverter. The introduction of Integral FCS is intended to minimize the steady-state error, which cannot be significantly reduced by FCS.

The implementation of IFCS in AC motor drives to analyze the steady-state error in d and q-axis currents was presented in [2]. Before the development of MPC techniques, conventional controllers such as PI, PD and PID were commonly used. In [3], the algorithms of the FCS and IFCS-MPC topologies for controlling various synchronous and asynchronous motor drives were designed and compared with conventional controllers.

A new FCS-MPC technique is proposed to regulate the flux dynamics of an induction motor [4]. In this control approach, the PWM technique is implemented to minimize the problems associated with the switching frequency. A comparative study between FCS and CCS method was highlighted in [5]. In this work, the execution methodology of both FCS and CCS action has been

discussed, such as modulation control and SVPWM control scheme, respectively. A predictive control strategy of an inverter-fed IM drive can be designed with current evaluation or with flux/torque evaluation [6].

This study provides the practical perception of MPC for inverter-fed drive systems. To diagnose the performance of IM, various strategies have been included, including field-oriented control, direct torque control, and predictive controllers [7]. Basically, optimization problems are assigned with specific cost functions depending on system parameters. In order to achieve fast dynamic behavior of the induction machine, innovative control strategies with two different objective functions for both torque and flux were defined [8]. In [9], an MPC scheme for direct flux control of induction motors with multiple three-phase structures was proposed to improve the fault-tolerant behavior of the drives by independently controlling the three phases.

The IFCS-MPC strategy for a single-phase Z-source inverter was implemented in [10] to compensate for the steady-state error caused by the FCS method.

FCS MPC has proven to be a promising control method for converter-powered IM drives. Two case studies of a converter-fed induction machine with and without an LC filter were analyzed in [11]. In [12], a predictive control approach is proposed to determine the length of the control horizon of an induction motor drive. As already discussed in previous literature, predictive control can be a fast-acting measure for optimal control of the switching states of inverters [13]. In general, a finite rule set based controller provides fast dynamic response and overcomes the limitations of traditional PI controllers. In [14], a deadbeat FCS topology was proposed for predictive current control to improve IM dynamics.

The adaptability, robustness and flexibility of the FCS technique has been compared with classical controllers [15] and a sliding mode based MPC method has been introduced for torque and flux control of induction motors [16],[17]. The field-oriented control of a three-phase induction motor by the FCS-MPC method with integrated forced control and DC control strategy is demonstrated in [18]. This algorithm can minimize the deviations between desired currents and predicted currents. Apart from single- or three-phase IM, the prediction mechanism has also provided a real control algorithm for multi-phase machines such as five-phase or six-phase machines [19-21] to optimize the machine performances.

A predictive phase angle controller was used to control the phase angles of the stator phase currents [22] and the overall properties of the machine were analyzed. The main aspects of controlling the dynamics of an induction machine are monitoring the flux and current behavior. Accordingly, observer-based predictive flux control [23] and various flux control strategies [24],[25] were implemented to observe and control the variations of machine parameters.

The development of MPC methods has increased much faster due to their reputation for responding quickly and providing a simple system algorithm. The many advantages of this novel technique include minimizing harmonic current and torque distortions [26], multi-objective optimization, and a fast fault-tolerant approach [27]. In the current scenario, predictive controls are significantly used in high-performance drive systems such as induction machines, synchronous machines, linear motors, reluctance motors and multi-phase machine drives [28]. In [29], a total disturbance observer-based PCC model of IM was presented, which directly incorporates the disturbance into the prediction mechanism, thus eliminating the need for a separate controller. The most recent advancement of MPC action features the fast-acting control mechanism of multi-phase induction motor drives [30],[31]. The application of model predictive control in power electronics increases the flexibility, robustness and speed of designed control architectures. To increase the dynamics, various predictive controllers are used, such as: Deadbeat controllers, hysteresis current controllers (HCC) and trajectory-based controllers. Predictive controls of machine drives are based on current or torque/flow control[32-34]. Although the FCS-MPC method adopted by researchers has largely improved the dynamic response of the system, the technique has drawbacks in terms of minimizing the steady-state error. Therefore, this work is motivated to apply the finite control set model (I-FCS-MPC) predictive control with integral action to further minimize the steady-state error and with a fast dynamic response. Therefore, two integral gain constants Kd and Kq are introduced in the control structure for direct and quadrature axis currents. Therefore, it is necessary to have the correct values of these two parameters to obtain a system with minimum steady state error and acceptable switching losses.

However, to evaluate the efficacy of IFCS-MPC and FCS-MPC, we have applied the Genetic Algorithm (GA) [35-37] and Gravitational Search Algorithm (GSA) [37-40] for comparison. The results show that both FCS-MPC and I-FCS-MPC methods exhibit superior performance in comparison to the GSA and GA algorithms. Despite the evolution of control strategies and the introduction of new techniques, the application of model predictive control in power electronics continually enhances the robustness, flexibility, and speed of designed control architectures. This work aims to build upon this foundation, exploring the potential of I-FCS-MPC in the realm of induction motor drives [41]. The optimal values for these parameters depend greatly on the specific problem being solved. However, here are some general guidelines for selecting the parameters: Inertial Mass: The inertial mass is typically calculated from the agent's fitness, so there's no initial value to set. However, it is common to normalize the fitness values so that the sum of all agents' inertial mass equals 1 at each iteration. Diminishing Gravitational Constant: The gravitational constant G is often initialized to a value such as 100 or 1 and reduced over time. A common approach is to decrease G linearly over the iterations.

The article is structured in the following manner to facilitate a comprehensive exploration of the implemented techniques. Section 2 introduces related reviews and research literature, setting a rich backdrop for the study. Moving ahead, Section 3 elaborates on the inverter topology, dynamic model, control methodologies, and the crucial algorithms designed for the proposed predictive controllers for an Induction Motor (IM) drive. This section also ventures into the structure and implementation of the Gravitational Search Algorithm (GSA) and the Genetic Algorithm (GA).

Section 4 is devoted to presenting and discussing the responses of torque, currents, and speeds with respect to step changes of the various proposed control actions. In Section 5, a comparative analysis is performed on the designed Model Predictive Controls (MPCs) with a focus on their torque and current dynamic characteristics. The paper finally concludes with Section 6, summarizing the main conclusions drawn from the study along with relevant references.

II. RELATED REVIEWS

In recent years, predictive control methods have become a pivotal area of interest for induction motor drives due to their

superior dynamic response and simplified implementation over traditional methods. [2] first introduced integral FCS predictive current control of induction motor drives, providing a basis for improving dynamic response and static error performance [2]. Subsequent research by introduced the application of PID and predictive control methods using MATLAB/Simulink, affirming the advantages of these predictive control approaches [3]. However, this work lacked an in-depth exploration of practical implementation challenges. Advancements in this field continued, who explored direct flux and current vector control, as well as Finite Control Set-Model Predictive Speed Control, respectively [4,5]. These studies validated the control principles and applications for high-performance drive systems [5].

The literature further expanded with comparative studies and explorations into various predictive control methods. contrasted current-based and flux/torque-based model predictive control methods for open-end winding induction motor drives, ultimately favoring the flux/torque-based method for its efficiency in reducing current ripple and improving dynamic response [6]. Advancing the topic, further explored advanced control strategies of induction machines: Field Oriented Control, Direct Torque Control, and Model Predictive Control [7]. The authors provided a detailed analysis and comparison of these strategies, indicating the dominance of Model Predictive Control in terms of performance. Similarly, presented a simple strategy for high-quality performance of AC machines using model predictive control [8], emphasizing the simplicity and effectiveness of Model Predictive Control. Concurrently, offered an in-depth analysis and comparison of advanced control strategies: Field Oriented Control, Direct Torque Control, and Model Predictive Control, with the latter emerging dominant [7]. This was further substantiated by, who touted the simplicity and effectiveness of Model Predictive Control [8].

More recently, research began exploring the intersection of predictive control methods with computational intelligence techniques, hybrid approaches, and innovative concepts. This includes studies such as those by F. Yahiaoui et al.[32], R. Venayagamoorthy et al.[33], Mehedi Ibrahim Mustafa et al. [34], T. Jalil et al.[35], J. Senthil Kumar et al.[36] and PA Naidu, V Singh[37] who utilized Genetic Algorithms and Gravitational Search Algorithm for optimizing the nonlinear control of induction motors. The introduction of these techniques has shown significant efficacy in performance enhancement. Meanwhile, , and Stando have extended model predictive control's application to power electronics, providing comprehensive design guidelines, exploring long-horizon control, and examining the constant switching frequency predictive control scheme [11,12,13,14]. Lastly, showcased an extended application of the predictive control concept to multi-phase systems [9]. In conjuction to this integration of predictive and optimal control algorithms for drive control established as a worthy dynamic platform [42],[43]. In essence, the ongoing research in the field emphasizes the diverse applications and continual advancements in predictive control methods for induction motor drives.

III. PROPOSED CONTROL METHODS

The working principle of model predictive control (MPC), where the variable of interest is the finite horizon control and is compared with the desired reference value to obtain the required command signal. This proposed work is based on simplifying the optimization of inverter states without PWM technique. Here, eight combinations of inverter states are formed as constraints for the control design. To better predict future behavior, the load model is used, hence the variables, which is why the name model predictive control arises. The optimization technique works on the principle of controlling the receding horizon. We can say that a constraint-free FCS-MPC method is similar to the discrete-time deadbeat feedback system, where the controller gain varies with time under the condition that the poles in the closed loop are at the origin of the complex plane.

To improve the steady-state behavior of the normal FCS-MPC method, an integral effect is added via a cascade control structure. The minimized objective function in the normal FCS-MPC method is just the squared difference between the predicted current and the measured current in the d-q reference frame. The main utility of the objective function in an I-FCS-MPC method is explicitly related to the sampling time Δt. Further two intelligent techniques such as Genetic Algrithm(GA) and Gravitational Search Algorithm(GSA) are introduced to evaluate the dynamic characteristics of designed Induction motor.

III. 1. MPC METHODOLOGY

MPC works with a finite horizon control principle. The controller or MPC block carries out the evaluation of control signals for a specific future point in time. Over time, the finite prediction horizon is updated by incorporating a future period and leaving behind a past period. Based on the predicted performance of the system, MPC generates a control sequence that is only applicable at the current sampling time.

After a sampling interval, the control sequence is changed based on the new measurements. In Figure 1, the red trajectory is the reference signal to follow. The green trajectory is the controlled signal obtained after proper measurements and manipulations at time k. The yellow curve is the past measure used to predict the future.

In the current state k, the MPC evaluates the control sequence for the prediction horizon, as indicated by the purple line. Similarly, at sampling time k+1, k+2, etc., MPC generates different sets of controlled sequences for their respective prediction horizons.

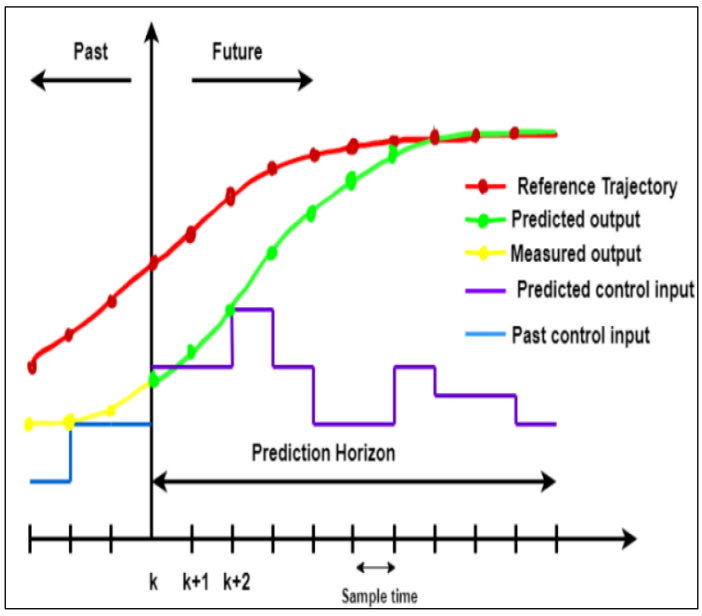

Figure 1: MPC with Predictive Horizon
Source: Authors, (2025).

III. 2. DYNAMIC FRAMEWORK OF IM

For our experimental setup in a simulation environment, we took a case of a squirrel cage type induction motor. The current and

torque dynamics are represented in the following mathematical equations with respect to the d-q reference frame [3].

$$\frac{di_{sd}}{dt} = -\frac{1}{\tau_\sigma} i_{sd} + \omega_s i_{sq} + \frac{k_r}{r_\sigma \tau_\sigma \tau_r} \varphi_{rd} + \frac{1}{r_\sigma \tau_\sigma} \quad (1)$$

$$\frac{di_{sq}}{dt} = -\omega_s i_{sd} - \frac{1}{\tau_\sigma} i_{sq} - \frac{k_r}{r_\sigma \tau_\sigma} \omega_e \varphi_{rd} + \frac{1}{r_\sigma \tau_\sigma} \quad (2)$$

$$\omega_s = \omega_e + \frac{L_h}{\tau_r} \quad (3)$$

$$\omega_s = \omega_e + \frac{1}{\tau_r} \frac{i_{sq}}{i_{sd}} \quad (4)$$

Where

i_{sd} & i_{sq} are the measured currents on the d-axis, q-axis, expressed in Ampere (A)

v_{sd} & v_{sq} are the measured voltages on the d-axis, q-axis, expressed in Volt (V)

ω_s, ω_e are the angular speed of the stator and rotor, expressed in rad/sec

φ_{rd}= d-axis Rotor flux (Wb)

All other parameters used in the IM drive dynamic equations are defined below[41-42].

Leakage factor:

$$\sigma = 1 - \frac{L_h^2}{L_s L_r} \quad (5)$$

Stator time constant:

$$\tau_s = \frac{L_s}{R_s} \quad (6)$$

Rotor time constant:

$$\tau_r = \frac{L_r}{R_r} \quad (7)$$

Coefficients:

$$k_r = \frac{L_h}{L_r} \quad (8)$$

$$r_\sigma = R_s + R_r k_r^2 \quad (9)$$

$$\tau_\sigma = \frac{\sigma L_s}{r_\sigma} \quad (10)$$

The torque produced by the magnetic field, commonly known as electromagnetic torque, is proportional to, $\varphi_{rd} i_{sq}$, which is expressed as

$$T_e = \frac{3}{2} Z_p \frac{L_h}{L_r} \varphi_{rd} i_{sq} \quad (11)$$

The mechanical parameters of the induction motor must be taken into account and derived from the general motor equation for rotation, which is given as follows:

$$J_m \frac{d\omega_m}{dt} + f_d \omega_m = T_e - T_L \quad (12)$$

Where $\omega_m(t)$, the mechanical Speed of the rotor ($\omega_m = \frac{\omega_e}{Z_p}$), J_m, the inertia of the motor and f_d, the coefficient of friction, T_e & T_L the torque in the electromagnetic field and the load. With consideration of the dynamics, the model and using the above in to the motion equation, representing in (12),

$$\frac{d\omega_m}{dt} = \frac{-f_d}{J_m} \omega_m + \frac{3}{2} \frac{Z_p L_h}{L_r J_m} \varphi_{rd} i_{sq} - \frac{T_L}{J_m} \quad (13)$$

The electrical speed of the rotor can be expressed as,

$$\frac{d\omega_e}{dt} = \frac{-f_d}{J_m} \omega_e + \frac{3}{2} \frac{Z_p^2 L_h}{L_r J_m} \varphi_{rd} i_{sq} - \frac{Z_p T_L}{J_m} \quad (14)$$

The physical and technical parameters previously defined and used in the IM model were considered and tabulated below for the evaluation of the system performance.

Table 1: 3-Φ IM model parameters.

Parameters	Values
Winding resistance offer to Stator(R_s)	111.2 Ohms
Winding resistance offer to Rotor(R_r)	88.3 Ohms
Winding inductance offer by Stator (L_s)	00.6155 Henrys
Winding inductance offer by Rotor (L_r)	00.6380 Henrys
Mutual inductance of Machine (L_h)	00.57 Henrys
Moment of inertia (J_m)	0.00176 Kgm^2
Friction viscous gain (f_d)	0.00038818 Nm/rad/sec
Number of Pole pairs(Zp)	2nos

Source: Authors, [3].

III. 3. MODELLING OF THREE PHASE INVERTER

We consider a 3φ inverter that converts 520V to 3φ AC for a squirrel cage type induction motor, whose physical parameters are shown in Table 1. The inverter operates in non-linear mode, discrete time system with 180° operating mode, 7 outputs and 8 configuration states. For simplicity and rounding, we ignore the IGBT saturation voltage and diode forward voltage drop when modeling and mathematically calculating the simulation. The schematic circuit as a voltage source and inverter to the 3-φ IM is shown below in Figure 2.

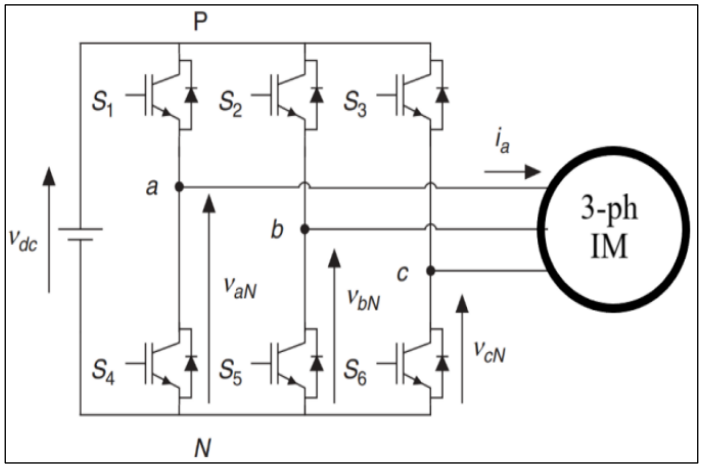

Figure 2: VSI fed 3-Φ IM.
Source: Authors, (2025).

The switching states for inverter action is specified with the reference of the gating signals *Sa*, *Sb*, *Sc* and can be represented as follows[1]:

$$S_a = \begin{cases} 1, \text{if } Switch_1 \text{ on and } Switch_4 \text{ off} \\ 0, \text{if } Switch_1 \text{ off and } Switch_4 \text{ on} \end{cases}$$

$$S_b = \begin{cases} 1, \text{if } Switch_2 \text{ on and } Switch_5 \text{ off} \\ 0, \text{if } Switch_2 \text{ off and } Switch_5 \text{ on} \end{cases}$$

$$S_c = \begin{cases} 1, \text{if } Switch_3 \text{ on and } Switch_6 \text{ off} \\ 0, \text{if } Switch_3 \text{ off and } Switch_6 \text{ on} \end{cases}$$

The concept of space vector modulation was adopted for voltage vectors with regard to optimal switching states [41],[42].

The generation of switching states results in eight voltage vectors listed in Table 2, which can be predicted by equation (15) as follows:

$$v = \frac{2}{3} V_{dc}(S_a + aS_b + a^2 S_c) \text{ Where, } a = e^{-j(2\pi/3)} = -\frac{1}{2} + j\frac{\sqrt{3}}{2}, \quad (15)$$

with a phase displacement of 120° , between any two phases.

Table 2: Switching states with voltage vectors.

Sa	Sb	Sc	Voltage Vector(v)
0	00	00	$\overrightarrow{v_0} = 0$
1	00	00	$\overrightarrow{v_1} = \frac{2}{3} v_{dc}$
1	11	00	$\overrightarrow{v_2} = \frac{1}{3} v_{dc} + j\frac{\sqrt{3}}{3} v_{dc}$
0	11	00	$\overrightarrow{v_3} = -\frac{1}{3} v_{dc} + j\frac{\sqrt{3}}{3} v_{dc}$
0	11	11	$\overrightarrow{v_4} = -\frac{2}{3} v_{dc}$
0	00	11	$\overrightarrow{v_5} = -\frac{1}{3} v_{dc} - j\frac{\sqrt{3}}{3} v_{dc}$
1	00	11	$\overrightarrow{v_6} = \frac{1}{3} v_{dc} - j\frac{\sqrt{3}}{3} v_{dc}$
1	1	1	$\overrightarrow{v_7} = 0$

Source: Authors, (2025).

The simple mathematical model of a three-phase inverter circuit that defines the generated output voltages (phase to neutral) by applying switching signals is shown in Figure 3. The optimal operation of prediction algorithms leads to the switching state listed in the Table. 2.

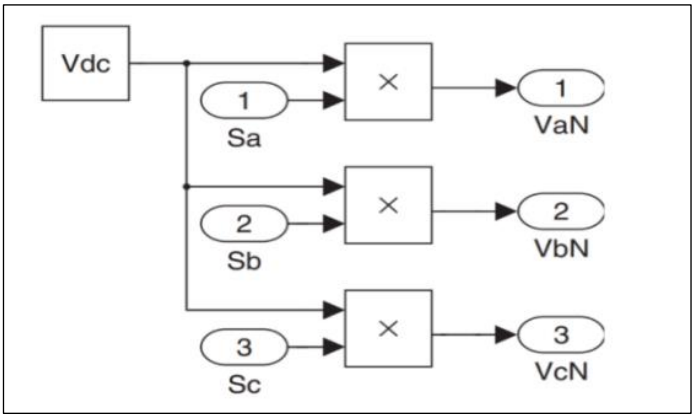

Figure 3: Generated Voltage of VSI.
Source: [1].

III. 3. PREDICTIVE CURRENT CONTROL

The predictive control algorithm can be organized in the following way.

1) The measurement of the reference current i*(ti+1) is carried out via the outer control loop, while the measurement of the load current i(t) must be carried out in each state with respect to the sampling interval.
2) The evaluation and prediction of the load current value for each upcoming sampling interval i(ti+1) taking into account the different voltage vector.
3) The cost function J uses the difference between the reference and the predicted currents of upcoming scanning frames with the corresponding voltage vector for the error calculation.

$$J=\{i_d^*(t_i)-i_d(t_{i+1})\}^2+\{i_q^*(t_i)-i_q(t_{i+1})\}^2 \quad (16)$$

4) The switching status signals generated minimize the current error and must be listed and taken into account for use.

In this algorithm, the previous value of the load current and the next state of the current leads to the prediction of 7 different states and 8 configurations for the operation of the inverter circuit. For each discrete state, we need to calculate the current value, predict it and compare it with the reference current to detect minimal errors and changes. We need to calculate for all 8 values listed in the table above and record the errors. The optimal operating states are fed to the inverter, which serves as a voltage source inverter. The flowchart of the above process is shown in Figure 4.

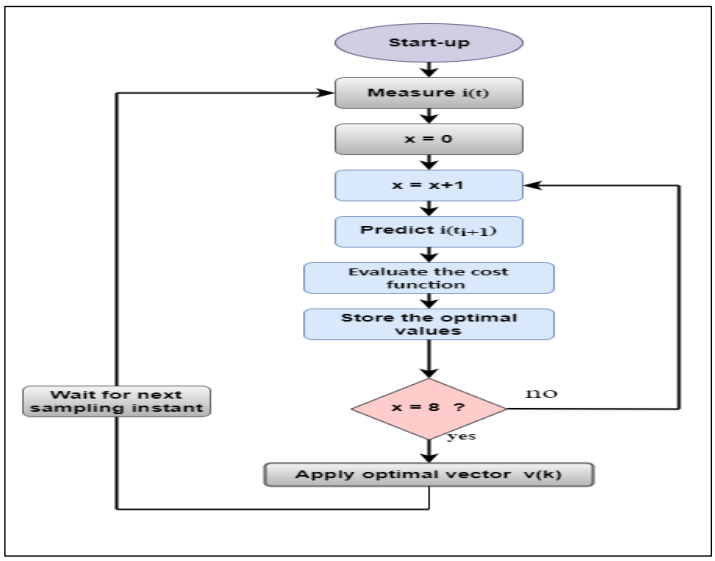

Figure 4: Flow Chart for Predictive Current Control.
Source: [41].

III. 4. FCS-MPC METHOD FOR IM

When generalizing the equations, predicted load currents in the d-q frame for sampling time ti can be derived from forward Euler approximations [1].

$$\frac{di_{sd}(t)}{dt} \approx \frac{i_{sd}(t_{i+1}) - i_{sd}(t_i)}{\Delta t} \quad (17)$$

$$\frac{di_{sq}(t)}{dt} \approx \frac{i_{sq}(t_{i+1}) - i_{sq}(t_i)}{\Delta t} \quad (18)$$

Where, Δt is the sampling interval,

$i_d(t_{i+1})$ and $i_q(t_{i+1})$ are predicted values of current on d-q frame, i_d^* and i_q^* are the desired values of current on the d-q frame.

Now by blending Equations (17) & (18) in Equations (1) & (2) respectively, the discrete differential equations transform as the difference equations and can be represented as follows:

$$i_{sd}(t_{i+1}) = i_{sd}(t_i) + \Delta t(-\frac{1}{\tau_\sigma} i_{sd}(t_i) + \omega_s i_{sq}(t_i) + \frac{k_r}{r_\sigma \tau_\sigma \tau_r} \varphi_{rd}(t_i) + \frac{1}{r_\sigma \tau_\sigma} u_{sd}(t_i)) \quad (19)$$

$$i_{sq}(t_{i+1}) = i_{sq}(t_i) + \Delta t(-\omega_s i_{sd}(t_i) - \frac{1}{\tau_\sigma} i_{sq}(t_i) - \frac{k_r}{r_\sigma \tau_\sigma} \omega_e(t_i)\, \varphi_{rd}(t_i) + \frac{1}{r_\sigma \tau_\sigma} u_{sq}(t_i)) \quad (20)$$

The prediction equations for current forecasting corresponding to Equation (19) and (20) can be presented in matrix form.

$$\begin{bmatrix} i_{sd}(t_{i+1}) \\ i_{sq}(t_{i+1}) \end{bmatrix} = (I + \Delta t A_m(t_i)) \begin{bmatrix} i_{sd}(t_i) \\ i_{sq}(t_i) \end{bmatrix} + \Delta t B_m \begin{bmatrix} u_{sd}(t_i) \\ u_{sq}(t_i) \end{bmatrix} + \begin{bmatrix} \frac{k_r \Delta t}{r_\sigma \tau_\sigma \tau_r} \varphi_{rd}(t_i) \\ -\frac{k_r \Delta t}{r_\sigma \tau_\sigma} \omega_e(t_i)\, \varphi_{rd}(t_i) \end{bmatrix} \quad (21)$$

Where,

I is a 2*2, identity matrix and

$$A_m(t_i) = \begin{bmatrix} -\frac{1}{\tau_\sigma} & \omega_s(t) \\ -\omega_s(t) & -\frac{1}{\tau_\sigma} \end{bmatrix}$$

$$B_m = \begin{bmatrix} \frac{1}{r_\sigma \tau_\sigma} & 0 \\ 0 & \frac{1}{r_\sigma \tau_{\sigma_q}} \end{bmatrix}$$

The block diagram of FCS-MPC Model used for 3-ph induction motor is illustrated in Figure 5.

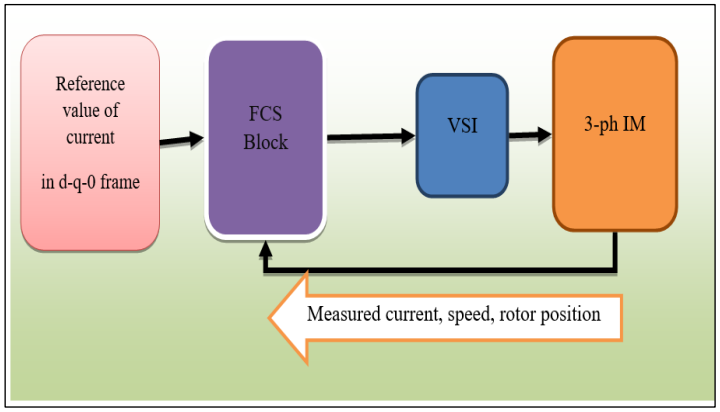

Figure 5: FCS-MPC Structure for IM Control.
Source: [41].

This method is processed in the following way.

1) The reference value is represented in d-q frame (idref and iqref).

2) Measured currents in d-q frame, velocity in radians per second and rotor angle position in radians are used as input to FCS control block .

3) The output of the FCS block is the switching states to the voltage link inverter.

4) The control output of the inverter is fed to the IM model as a voltage source.

5) In this article, a two-stage three-phase VSI is considered for the application of prediction schemes. Since all modeling and calculation is done in the d-q-0 reference frame, the generated stress vectors must be transformed from the a-b-c coordinate to the d-q-0 coordinate using the Park transform.

$$\begin{bmatrix} u_{sd} \\ u_{sq} \end{bmatrix} = \frac{2}{3} \begin{bmatrix} cos\theta & \cos(\theta - \frac{2\pi}{3}) & \cos(\theta + \frac{2\pi}{3}) \\ -sin\theta & -\sin(\theta - \frac{2\pi}{3}) & -\sin(\theta + \frac{2\pi}{3}) \end{bmatrix} \begin{bmatrix} V_{an} \\ V_{bn} \\ V_{cn} \end{bmatrix} \quad (22)$$

Where,

u_{sd} = d-axis Voltage,

u_{sq} = q-axis Voltage,

θ = Rotor angle

V_{an} ,V_{bn},V_{cn} are the phase to neutral voltages,

V_{dc} = Input DC voltage to VSI

In the FCS-MPC approach, there are seven sets and values are presented based on the rotor angular position and sampling time. In this control strategy, we employ the objective function, which is defined as the sum of the square of the error difference between the desired and predicted current values in the d-q frame. The objective function J takes into account the variables measured with the sampling time and the manipulated variables. Equation (16) can be expressed as follows:

$$J_K = \left(i^*_{sd}(t_i) - i_{sd}(t_i) - \Delta t(-\frac{1}{\tau_\sigma} i_{sd}(t_i) + \omega_s i_{sq}(t_i) + \frac{k_r}{r_\sigma \tau_\sigma \tau_r} \varphi_{rd}(t_i) + \frac{1}{r_\sigma \tau_\sigma} u_{sd}(t_i)) \right)^2 + \left(i^*_{sq}(t_i) - i_{sq}(t_i) - \Delta t(-\omega_s i_{sd}(t_i) - \frac{1}{\tau_\sigma} i_{sq}(t_i) - \frac{k_r}{r_\sigma \tau_\sigma} \omega_e(t_i)\, \varphi_{rd}(t_i) + \frac{1}{r_\sigma \tau_\sigma} u_{sq}(t_i)) \right)^2 \quad (23)$$

Where ,

φ_{rd} = d-axis rotor flux and

K = index from 0 to 7.

The principle of declining horizon control is used here, which is based on feedback parameters such as: $i_{sd}(t_i)$, $i_{sq}(t_i)$, ω_e and θ_e, and the 3-ph IM model predicts a value for one step ahead. The objective function is calculated based on the above feedback values, parameters of the 3-ph IM model and the $u_{sd} - u_{sq}$ value pair. Seven sets of objective functions are calculated based on seven pairs of $u_{sd} - u_{sq}$ values. The index value is 0 or 7, it is determined based on the previous states of the inverter. The switching combinations and corresponding voltage vectors used in the FCS-MPC technique are listed in Table 3.

Table 3: Switching States and Voltage Vectors of FCS Block.

Switching State			Voltage Vector	Phase Voltage		
Sa	Sb	Sc	v	V_{an}	V_{bn}	V_{cn}
0	0	0	$\vec{v_0}$	$-\frac{V_{dc}}{2}$	$-\frac{V_{dc}}{2}$	$-\frac{V_{dc}}{2}$
1	0	0	$\vec{v_1}$	$\frac{V_{dc}}{2}$	$-\frac{V_{dc}}{2}$	$-\frac{V_{dc}}{2}$
1	1	0	$\vec{v_2}$	$\frac{V_{dc}}{2}$	$\frac{V_{dc}}{2}$	$-\frac{V_{dc}}{2}$
0	1	0	$\vec{v_3}$	$-\frac{V_{dc}}{2}$	$\frac{V_{dc}}{2}$	$-\frac{V_{dc}}{2}$
0	1	1	$\vec{v_4}$	$-\frac{V_{dc}}{2}$	$\frac{V_{dc}}{2}$	$\frac{V_{dc}}{2}$
0	0	1	$\vec{v_5}$	$-\frac{V_{dc}}{2}$	$-\frac{V_{dc}}{2}$	$\frac{V_{dc}}{2}$
1	0	1	$\vec{v_6}$	$\frac{V_{dc}}{2}$	$-\frac{V_{dc}}{2}$	$\frac{V_{dc}}{2}$
1	1	1	$\vec{v_7}$	$\frac{V_{dc}}{2}$	$\frac{V_{dc}}{2}$	$\frac{V_{dc}}{2}$

Source: Authors, (2025).

The phase-neutral voltages of each phase can be defined in relation to the switching states and the DC input voltage of the inverter as follows:

$$\begin{bmatrix} V_{an} \\ V_{bn} \\ V_{cn} \end{bmatrix} = \begin{bmatrix} S_a - \frac{1}{2} \\ S_b - \frac{1}{2} \\ S_c - \frac{1}{2} \end{bmatrix} \mathrm{V_{dc}} \quad (24)$$

III. 5. IFCS-MPC METHOD FOR IM

The IFCS-MPC method uses the same concept as the normal FCS-MPC method, but different in control effect, so in the I-FCS-MPC method the objective function is variable with respect to voltage signals, while in the normal FCS -MPC method the same applies was formed in relation to current signals. The optimal control signals obtained from the feedback control framework are given as follows:

$$\begin{bmatrix} u_{sd}(t_i)^{opt} \\ u_{sq}(t_i)^{opt} \end{bmatrix} = K_{fcs} \left(\begin{bmatrix} {i_{sd}}^*(t_i) \\ {i_{sq}}^*(t_i) \end{bmatrix} - \begin{bmatrix} i_{sd}(t_i) \\ i_{sq}(t_i) \end{bmatrix} \right) \quad (25)$$

Where, K_{fcs} is the gain of the controller and can be calculated from Equation (21) as:

$$K_{fcs}(t_i) = (\Delta t^2 \mathrm{B_m^T B_m})^{-1} \mathrm{B_m^T} \Delta t \, (\mathrm{I} + \Delta t A_m(t_i)) \quad (26)$$

Further modifying by putting the matrix form of A_m & $\mathrm{B_m}$,

$$K_{fcs}(t_i) = \begin{bmatrix} \frac{r_\sigma \tau_\sigma}{\Delta t}(1 - \frac{\Delta t}{\tau_\sigma}) & \omega_s(t_i) r_\sigma \tau_\sigma \\ -\omega_s(t_i) r_\sigma \tau_\sigma & \frac{r_\sigma \tau_\sigma}{\Delta t}(1 - \frac{\Delta t}{\tau_\sigma}) \end{bmatrix} \quad (27)$$

Utilizing the integral action in discrete time control system, Equation (25) can be updated as:

$$\begin{bmatrix} u_{sd}(t_i)^{opt} \\ u_{sq}(t_i)^{opt} \end{bmatrix} = K_{fcs}(t_i) \begin{bmatrix} \frac{K_d}{1-q^{-1}} ({i_{sd}}^*(t_i) - i_{sd}(t_i)) \\ \frac{K_q}{1-q^{-1}} ({i_{sq}}^*(t_i) - i_{sq}(t_i)) \end{bmatrix} - \begin{bmatrix} i_{sd}(t_i) \\ i_{sq}(t_i) \end{bmatrix} \quad (28)$$

Where 'K_d' and 'K_q' are the of integral gains selected for current error at both d-axis and q-axis respectively, and $0 < Kd \leq 1$ and $0 < Kq \leq 1$ and $\frac{1}{1-q^{-1}}$ represents an integrator.

Now at sampling time t_i the optimum voltage signals are evaluated as:

$$\begin{bmatrix} u_{sd}(t_i)^{opt} \\ u_{sq}(t_i)^{opt} \end{bmatrix} = \begin{bmatrix} u_{sd}(t_{i-1})^{opt} \\ u_{sq}(t_{i-1})^{opt} \end{bmatrix} + K_{fcs}(t_i) \begin{bmatrix} K_d \, ({i_{sd}}^*(t_i) - i_{sd}(t_i)) \\ K_q \, ({i_{sq}}^*(t_i) - i_{sq}(t_i)) \end{bmatrix} - K_{fcs}(t_i) \begin{bmatrix} \Delta i_{sd}(t_i) \\ \Delta i_{sq}(t_i) \end{bmatrix} \quad (29)$$

The upgraded objective function for I-FCS-MPC is defined as

$$J_K = \frac{\Delta t^2}{(r_\sigma \tau_\sigma)^2} (u_{sd}(t_i)^K - u_{sd}(t_i)^{opt})^2 + \frac{\Delta t^2}{(r_\sigma \tau_\sigma)^2} (u_{sq}(t_i)^K - u_{sq}(t_i)^{opt})^2 \quad (30)$$

This is the objective function that is calculated for each control with index K = 0, 1, 2, ……, 6. The index value and the corresponding control set for which the target function is minimal are selected for generating the respective switching pulse to the inverter. The schematic of I-FCS-MPC for IM is shown in Figure 6.

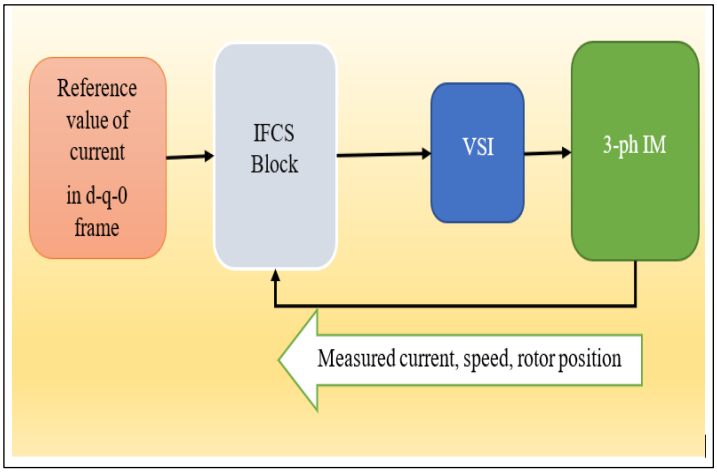

FIgure 6: Structure of I-FCS-MPC for IM.
Source: [43].

The control architecture of I-FCS-MPC for a three-phase induction motor with integral gain parameters and optimal voltage vectors is shown in Figure 7. From the block diagram shown below, we can visualize the control structure of the predictive current controller in the d-q reference frame. In addition, the mathematical representation of the previously defined equation (28) is demonstrated. By further modifying with gain parameters, equation (29) is extracted for optimal evaluation of the integral FCS control mechanism. In the implemented control algorithm, the values of the integral gain parameters *Kd* and *Kq* are set to 0.1 [3]. Further analysis can also be performed by using different values of the gain parameters ranging from 0 to 1.

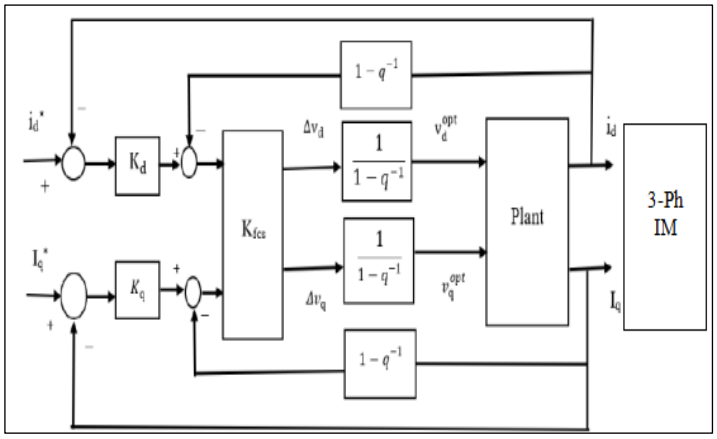

Figure 7: Control Architecture of Proposed I-FCS-MPC.
Source: [42].

III. 6. STRUCTURING GSA & GA FOR IM

The application of metaheuristic algorithms such as the Gravitational Search Algorithm (GSA) and Genetic Algorithm (GA) to the problem of induction motor control brings an innovative approach to system optimization. In GSA, the search agents are considered as objects and their performance is measured by their masses, which directly influence the gravitational attraction. This provides a balance between exploitation and exploration capabilities, thereby facilitating effective search of the optimal solution space.

In comparison, the GA employs biological evolutionary concepts including selection, crossover, and mutation to explore the solution space. The effectiveness of GA lies in its ability to handle a diverse population and evolve it over time to find optimal

or near-optimal solutions. Both GSA and GA, due to their stochastic nature, have the potential to avoid being trapped in local minima, making them particularly suitable for the nonlinear and complex problem of induction motor control. Their effectiveness is deeply tied to the proper tuning of algorithmic parameters those are mentioned in Table. 4.

Table 4.Parameter constraints used for GSA and GA.

GSA Parameters	GA Parameters
Population size (pop_size) = 50	Population size (pop_size) 50
Gravitational constant (G) = set to 100 or 1	Number of generations (ngen) = 100-500
lower and upper bounds = [0,0]-[10/400,10/400]	lower and upper bounds = [0,0]- [10/400,10/400]
Masses of agents = fitness function	Crossover rate = 0.5
Inertia weight = 0.4	Mutation rate (mutpb) =0.2
Diminishing gravitational constant = G	Crossover operator = *(DEAP library)
Distance calculation = Euclidean distance	Selection method
	Tourn-size = 3

Source: Authors, (2025).

III. 7. APPLYING ALGORITHMSON IM DYNAMICS.

1. GSA Algorithm

Step-1: Initialize a population of agents with random positions and velocities in the search space (problem space).
Step-2: Compute the fitness of each agent by taking motor dynamic parameters.
Step-3: Based on the fitness, assign a mass value to each agent - the better the fitness, the higher the mass.
Step-4: Calculate the force between each pair of agents/pop.
Step-5: Update the velocity and position of each agent based on the computed forces.
Step-6: Repeat these steps until a termination criterion is met (such as a maximum number of iterations or an acceptable solution has been found).

2. GA Algorithm

Step-1: Initialize a population of individuals with random genotypes.
Step-2: Define a fitness function of each particle by taking motor dynamic parameters.
Step-3: Select individuals for reproduction based on their fitness - the better the fitness, the higher the probability of selection.
Step-4: Apply crossover and mutation operators to the selected individuals to generate offspring for the next generation.
Step-5: Replace the current population with the offspring to form a new generation.
Step-6: Repeat these steps until a termination criterion is met.

Gravitational Search Algorithm (GSA) and Genetic Algorithm (GA) have gained prominence as effective strategies in the intelligent control methodologies for induction motor drives. GSA functions through initializing a population of agents, each with random velocities and positions, within the problem space. An assigned mass value to each agent, proportional to its fitness, facilitates the inter-agent dynamics based on gravitational forces, thereby updating their velocities and positions. This algorithm persists until meeting a termination criterion, such as finding an acceptable solution or reaching a maximum iteration limit. Simultaneously, GA operates by initiating a set of individuals with random genotypes. A predefined fitness function evaluates these individuals' problem-solving proficiency. Individuals with higher fitness have an increased likelihood of reproduction selection. The offspring, derived from crossover and mutation operations, create the new generation, and this algorithm also continues until a termination criterion is met. When applied to induction motors, these algorithms can optimize performance parameters like minimizing energy consumption, enhancing response times, or refining speed and torque control precision.

Nevertheless, the performance of these algorithms relies on the unique characteristics of the induction motor and the specifics of the control problem, necessitating careful tuning and adaptation of these methodologies for optimal induction motor drive control.

IV. RESULTS AND DISCUSSIONS

The previously mentioned three-phase induction motor with the specified parameters was modeled and executed with the FCS, I-FCS, GSA and GA control algorithms applied to the inverter circuit. The dynamic characteristics of currents, torque and angular velocity of IM were analyzed for different prediction schemes implemented here. The total simulation and sampling time is set to 0.2 s and 80 μs, respectively.

IV. 1. CURRENT DYNAMIC CHARACTERISTICS

The reference currents in d-q frame for dynamic analysis have been depicted in Figure 8. The d-axis current is set to be a constant value of i_{sd} = 0.8A and q-axis current is taken to be a step signal of amplitude i_{sq}=3A with step changes at 0.1 sec to fix the value as 1A.

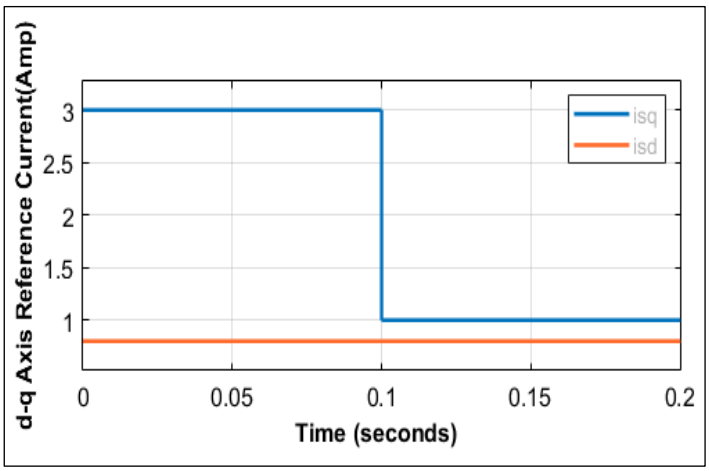

Figure 8: Three phase reference current in d-q frame.
Source: Authors, (2025).

Regarding the d-q axis currents and the change of rotor angle (θ), the characteristics of the desired currents in three phase sizes also change at a given time. These flows can be set as a reference for the flows in the next execution cycle and are used as a benchmark for all proposed approximations. The output currents

in d-q form obtained by the implemented MPC techniques are shown in Figure 9 and Figure 10, respectively.

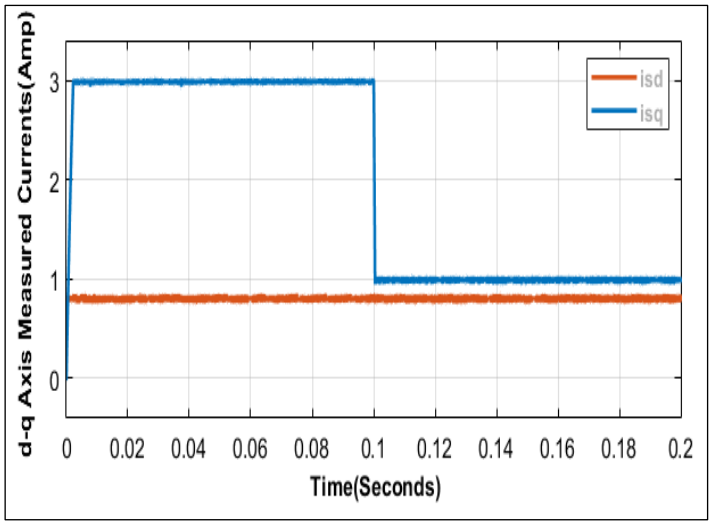

Figure 9: d-q axis currents of FCS-MPC Method.
Source: Authors, (2025).

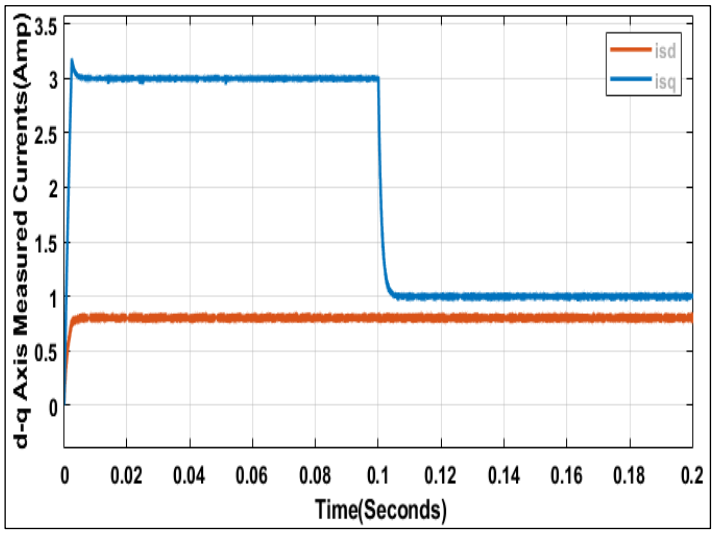

Figure 10: Output Currents of IFCS-MPC Method.
Source: Authors, (2025).

In the study of rotor angle (θ) dynamics and d-q axis currents, the use of the Gravitational Search Algorithm (GSA) and the Genetic Algorithm (GA) plays in meta-heuristic way. The intricacy of this dynamic is found in the immediate effect that the shifts in θ have on the characteristics of the currents in the three-phase quantities. For the subsequent execution cycle, a fundamental assumption is put forward: the currents as determined by the model will act as the reference point.

This benchmark is based on the results derived from the application of the GSA and GA techniques. To present a more tangible understanding of the impact of these methodologies, the output currents are visually represented. Figure 11 illustrates the output currents in d-q form, a result of applying the GSA technique, while Figure 12 displays thed-q form of output currents, an outcome attributed to the GA technique. Consequently, these figures offer a clearer comprehension of the influence of GSA and GA in the modelling of currents with comparison of FCS and I-FCS method.

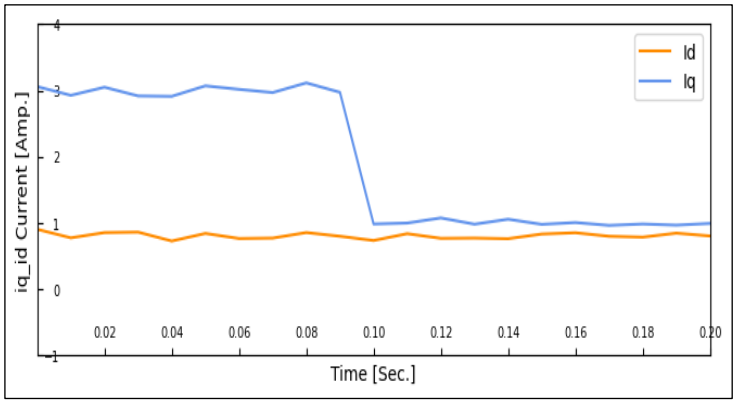

Figure 11: d-q axis currents of GSA Method.
Source: Authors, (2025).

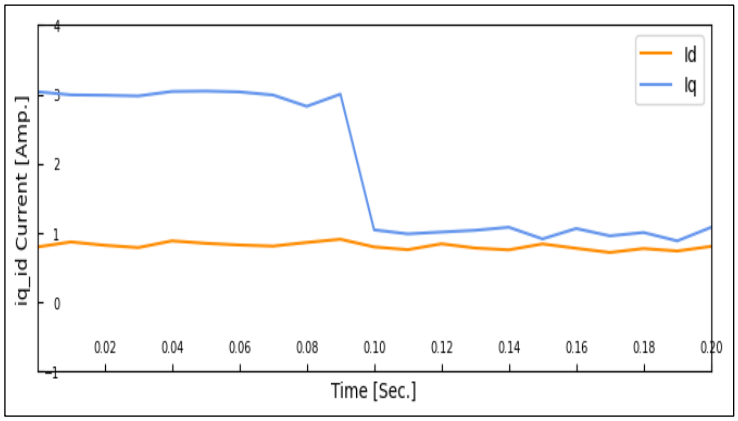

Figure 12: d-q axis currents of GA Method
Source: Authors, (2025).

IV.2. TORQUE & SPEED CHARACTERISTICS

Equation. (11) clearly demonstrates that electrical torque output (T_e) is a function of q-axis current and rotor flux of an induction motor. Hence it can be stated that the behaviour of q-axis current controls the torque characteristics. The plots of reference load torque (Figure 13) and output torque obtained from FCS and I-FCS predictive control schemes are depicted in Figure 14 & Figure 15 respectively. The load torque applied to the induction motor drive is a step signal of amplitude 2Nm with step changes at time 0.1second to 1Nm .

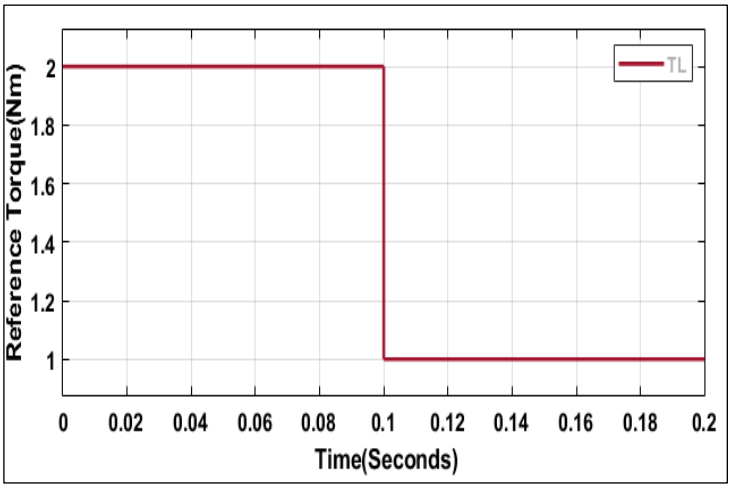

Figure 13: Load toque applied to the 3-ph IM model.
Source: Authors, (2025).

From the previous analysis, we can see that the electromagnetic torque output, quadrature axis current, rotor flux and angular velocity are dependent parameters. A change in the behavior of one of the mentioned parameters changes the properties of others, which directly affects the machine performance. Therefore, by controlling the current, we can regulate the torque and thereby also control the angular velocity of the motor in coordination with other dependent parameters. This concept can be defined mathematically by equations (13) and (14). Below, the angular velocity response of the induction motor is presented by corresponding step change in load torque and q-axis current for both proposed predictive controllers.(Figure 18).

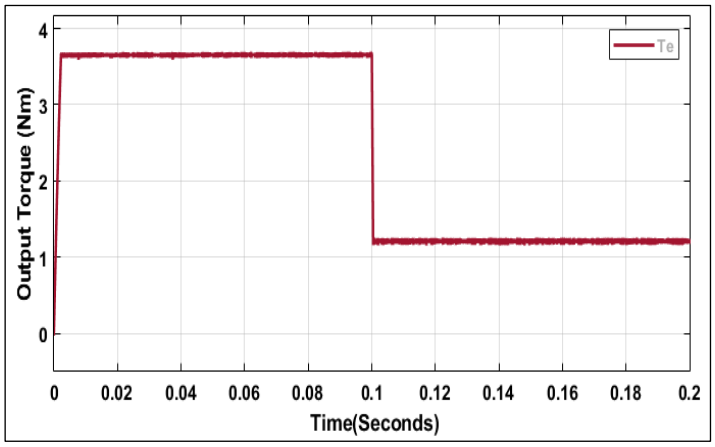

Figure 14: Torque output of FCS-MPC Method.
Source: Authors, (2025).

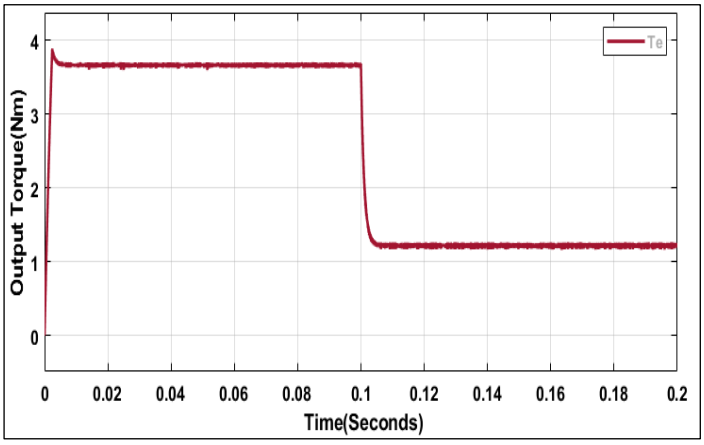

Figure 15: Torque output of I-FCS-MPC Method.
Source: Authors, (2025).

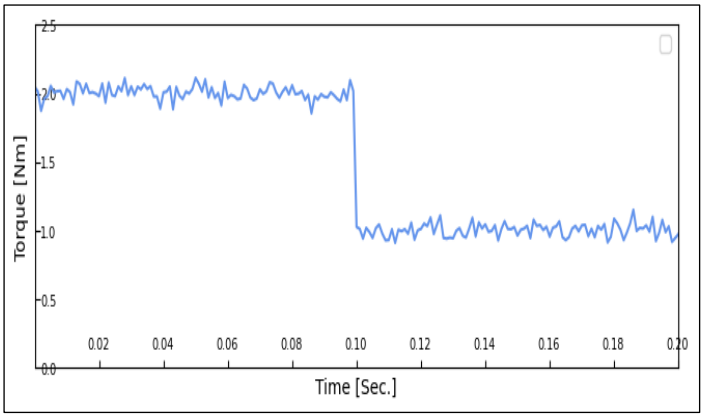

Figure 16: Torque output of GSA method.
Source: Authors, (2025).

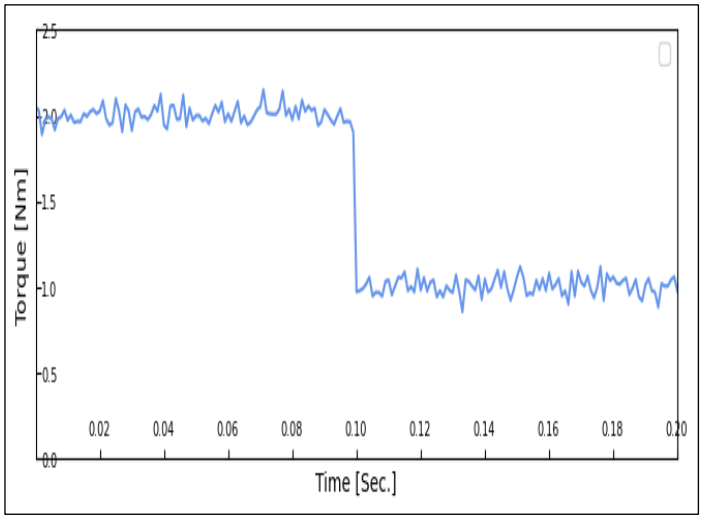

Figure 17: Torque output of GA method.
Source: Authors, (2025).

In our prior analysis, a change in one parameter invariably affects the others, setting off a cascade of impacts that influence the overall motor performance. This understanding introduces a strategic opportunity to manipulate the current and thus regulate torque as you can visualize on Figure 16 & Figure 17, and by extension, the angular speed of the motor. However, this control isn't a standalone process; it works in tandem with other dependent parameters, as succinctly demonstrated by Equations (13) & (14).

Implementing advanced algorithms such as the Gravitational Search Algorithm (GSA) and the Genetic Algorithm (GA) illuminates these complex dynamics, allowing for a deep exploration of the angular speed response of the induction motor to respective changes in load torque and q-axis current. Yet, it is worth noting that the Finite Control Set (FCS) and Integral Control Set (I-FCS) methods produce even more favorable results than the GSA and GA methods.

This observation is clearly visualized in Figure 18, which showcases the angular speed characteristics achieved by the GSA, GA, FCS, and I-FCS control approaches. Thus, these visualizations emphasize the superior efficacy of the FCS and I-FCS methods in optimizing motor performance through the effective management of interconnected parameters.

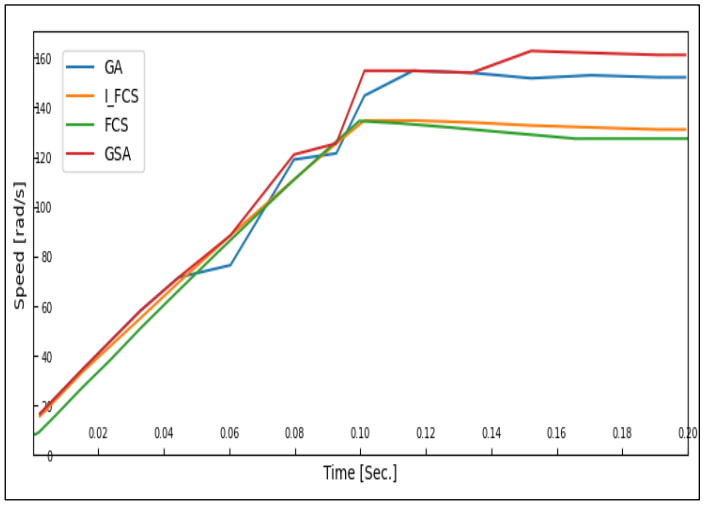

Figure 18: Angular Speed of FCS-MPC, I-FCS, GSA and GA.
Source: Authors, (2025).

The model outputs of currents, torque, angular velocity and rotor angle (Figure 19) of the designed induction motor drive were collected for optimal performance evaluation. The current dynamics are studied using a reference step signal of the quadrature axis current. Accordingly, the machine's electromagnetic torque output also follows the applied step load torque since the output torque is a function of the q-axis current and rotor flux defined in the equation. (11). Since the rotor position angle is updated after each point in time, the corresponding angular velocity also changes. Here, the step responses of current, torque and speed achieved by FCS and I-FCS control strategies were demonstrated. Currents and torque ripples can be visualized from the output reactions. It can be found that the ripple magnitudes for both current and torque output are lower for I-FCS-MPC compared to FCS-MPC, GSA and GA. Compared to the integral FCS technique, somewhat larger fluctuations in the speed response are also observed with FCS. Based on the model results of the implemented MPC strategies, a performance comparison was carried out in terms of d and q axis current responses, torque & speed trajectories and rotor angle deviations w.r.t step input signal. Further controller selection can be done by observing the current errors noted.

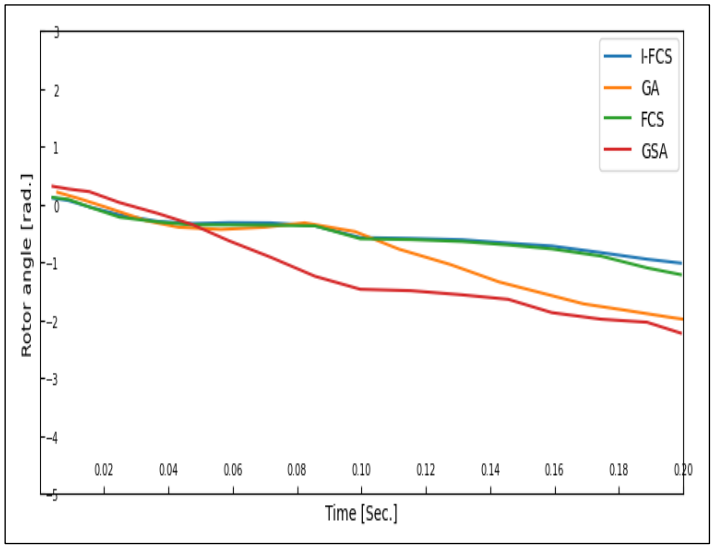

Figure 19: Rotor angle of FCS-MPC, I-FCS, GSA and GA.
Source: Authors, (2025).

In the pursuit of optimal performance, a thorough evaluation of the designed induction motor drive model reveals the significance of certain parameters - currents, torque, angular speed, and most importantly, the rotor angle (θ). These variables play pivotal roles in the complex dynamics of motor operation. The study of current dynamics, undertaken via a reference step signal of the quadrature axis current, emerges as a particularly engaging aspect. Notably, this signal has a profound influence on the rotor angle output of the machine, painting a picture of the intricate interdependency within the system. Furthermore, every update to the rotor position angle induces a corresponding shift in the angular speed, highlighting the delicate balance within these dynamics.

Crucially, when we employ the Integral Finite Control Set Model Predictive Control (I-FCS-MPC) approach, we observe a superior level of control over these dynamics when compared to the Finite Control Set Model Predictive Control (FCS-MPC), Gravitational Search Algorithm (GSA), and Genetic Algorithm (GA) methods. This key observation underscores the outstanding efficacy of the I-FCS-MPC approach in optimizing both the rotor angle control and the overall performance of the induction motor drive, thereby proving it to be a preferred strategy for motor control.

IV.3. COMPARISON OF PROPOSED CONTROLLERS

The simulation of FCS-MPC, I-FCS-MPC, GA and GSA optimized models is implemented with a sampling time of 80 microseconds. Two main factors that determine the characteristic results of the predictive controllers are the sampling time and an integral gain constant *Kd* and *Kq*. The integral gain is only applicable to the I-FCS-MPC method. At higher values of the integral gains, the current curves will overshoot in steady state with good performance. If we keep the integral gain low, dynamic overshoot can be compensated. Here the value of the integral profits is assumed to be 0.1. The sampling time does not have a large impact on dynamic performance. Its effect mainly concerns the steady state ripple. With a higher sampling time, the ripple is larger and therefore it is necessary to shorten the sampling time. However, the computing effort and switching losses of the inverter limit the sampling time to fall below a certain value. Therefore, a compromise is made between the allowable ripple and the computing time and the switching loss.

Table 5: Absolute Current Error.

	Absolute Current Error (in Amp)	
Control Technique	$\lvert I_{dRef} - I_{dMeas} \rvert$	$\lvert I_{qRef} - I_{qMeas} \rvert$
FCS-MPC	0.05226	0.06012
I-FCS-MPC	0.01641	0.02693
GA	0.44594	0.37549
GSA	0.36649	1.07919

Source: Authors, (2025).

From the obtained characteristics of currents and torque by the simulated control algorithms the responses of d and q axis current can be specified. As discussed earlier the ripples contents are observed to be significantly less in case of predictive controllers as compared to GA & GSA methods. Also it can be clearly demonstrated from Table 5 regarding the absolute current errors measured by different control techniques applied. Integral FCS scheme inherently performs superior to other intelligent techniques such as GA & GSA.

IV. CONCLUSIONS

The utility of induction motor drives in various industries such as traction, process, manufacturing and mining is significant. They play a central role in these areas due to their integral role in the development of electromagnetic torque and the dynamics of the converter-fed voltage. While there are several methods for speed and torque control, such as traditional PI, PID and hysteresis controllers, the Finite Control Set Model Predictive Control (FCS-MPC) method has a significant improvement in handling non-linear loads due to its predictive properties shown. This already promising method has been further improved with the implementation of the Gravitational Search Algorithm (GSA) and Genetic Algorithm (GA), adding another dimension to the study of the dynamics of 3-phase induction motors (IM). By adjusting the reference current in the q-axis and the reference load torque as step functions, we can observe the dynamic behavior of the 3-phase IM in more detail.

Although FCS-MPC, GSA and GA have shown notable strengths in IM control, Integral Finite Control Set Model

Predictive Control (IFCS-MPC) has shown superior performance in several aspects. With its similar control strategy to FCS-MPC, IFCS-MPC inherently reduces steady-state errors, improves slew rates, and provides superior trajectories with respect to the step input signal. Although the velocity responses of FCS-MPC and IFCS-MPC are similar, IFCS-MPC has fewer waves compared to FCS-MPC. The adaptive and flexible nature of MPC methods makes these controllers superior options in the modern control landscape. With just a few changes, IFCS-MPC outperforms GSA and GA, cementing its place as the preferred choice for modern control systems. Extending this predictive control approach can potentially revolutionize applications in electric vehicles, FACTS devices, and various energy system controls.

VI. AUTHOR'S CONTRIBUTION

Conceptualization: Shaswat Chirantan, Bibhuti Bhusan Pati
Methodology: Shaswat Chirantan, Bibhuti Bhusan Pati
Investigation: Shaswat Chirantan, Bibhuti Bhusan Pati
Discussion of results: Shaswat Chirantan, Bibhuti Bhusan Pati
Writing – Original Draft: Shaswat Chirantan
Writing – Review and Editing: Shaswat Chirantan, Bibhuti Bhusan Pati
Resources: Shaswat Chirantan, Bibhuti Bhusan Pati
Supervision: Shaswat Chirantan, Bibhuti Bhusan Pati
Approval of the final text: Shaswat Chirantan, Bibhuti Bhusan Pati

VII. ACKNOWLEDGMENTS

The authors would like to thank Veer Surendra Sai University of Technology, Burla, Sambalpur, India for facilitating this work.

VIII. REFERENCES

[1] Rodriguez, J. and Cortes, P.: "Predictive Control of Power Converters and Electrical Drives", John Wiley & Sons Ltd, United Kingdom, (2012)

[2] Wang L, Gan L. "Integral FCS predictive current control of induction motor drive. IFAC Proceedings Volumes". 2014 Jan 1;47(3):pp. 11956-11961.

[3] Wang L, Chai S, Yoo D, Gan L, Ng K. "PID and predictive control of electrical drives and power converters using MATLAB/Simulink". JohnWiley & Sons; 2015 Mar 2. pp. 171-205.

[4] Odhano S, Bojoi R, Formentini A, Zanchetta P, Tenconi A. "Direct flux and current vector control for induction motor drives using model predictive control theory". IET Electric Power Applications. 2017 Sep 4;11(8): pp. 1483-1491.

[5] Ahmed A.A., Koh, B.K., Kim, J.S. and Lee, Y.I., (2017). "Finite control set-model predictive speed control for induction motors with optimal duration". Proc. IFAC Papers On Line, Vol. 50(1), pp.7801-7806.

[6] Zhu B, Rajashekara K, Kubo H. "Comparison between current-based and flux/torque-based model predictive control methods for open-end winding induction motor drives". IET Electric Power Applications. 2017 Sep 4;11(8):pp. 1397-1406.

[7] Wang F, Zhang Z, Mei X, Rodriguez J, Kennel R. "Advanced control strategies of induction machine: Field oriented control, direct torque control and model predictive control". Energies. 2018 Jan;11(1):1-13.

[8] Norambuena M, Rodriguez J, Zhang Z,Wang F, Garcia C, Kennel R. "A very simple strategy for high-quality performance of AC machines using model predictive control". IEEE Transactions on Power Electronics. 2018 Mar 9;34(1):pp. 794-800.

[9] Rubino S, Bojoi R, Odhano SA, Zanchetta P. "Model predictive direct flux vector control of multi-three-phase induction motor drives". IEEE Transactions on Industry Applications. 2018 Apr 23;54(5):pp 4394-4404.

[10] Ramirez RO, Espinoza JR, Baier CR, Rivera M, Villarroel F, Guzman JI, Melin PE. "Finite-state model predictive control with integral action applied to a single phase Z-source inverter". IEEE Journal of Emerging and Selected Topics in Power Electronics. 2018 Sep 18;7(1):pp. 228-239.

[11] Karamanakos P, Geyer T. "Guidelines for the design of finite control set model predictive controllers". IEEE Transactions on Power Electronics. 2019 Nov 19;35(7):pp. 7434-7450.

[12] Wróbel, Karol Tomasz, Krzysztof Szabat, and Piotr Serkies. "Long-horizon model predictive control of induction motor drive." Archives of Electrical Engineering (2019): 579-593.

[13] Stando D, Kazmierkowski MP. Constant switching frequency predictive control scheme for three-level inverter-fed sensorless induction motor drive. Bulletin of the Polish Academy of Sciences. Technical Sciences. 2020;68(5).

[14] Wang, Junxiao, and Fengxiang Wang. "Robust sensor less FCS-PCC control for inverter-based induction machine systems with high-order disturbance compensation". Journal of Power Electronics (2020): pp. 1222-1231.

[15] Ortombina L, Karamanakos P, Zigliotto M. "Robustness Analysis of Long-Horizon Direct Model Predictive Control: Induction Motor Drives". IEEE 21st Workshop on Control and Modeling for Power Electronics (COMPEL) 2020 Nov 9 (pp. 1-8).

[16] Zhang, Yanqing, Zhonggang Yin, Wei Li, Jing Liu, and Yanping Zhang. "Adaptive sliding-mode-based speed control in finite control set model predictive torque control for induction motors." IEEE Transactions on Power Electronics 36, no. 7 (2020): 8076-8087.

[17] Kiani B, Mozafari B, Soleymani S, Mohammadnezhad Shourkaei H. Predictive torque control of induction motor drive with reduction of torque and flux ripple. Bulletin of the Polish Academy of Sciences. Technical Sciences. 2021; 69(4).

[18] Ali, Anmar Kh, and Riyadh G. Omar. "Finite control set model predictive direct current control strategy with constraints applying to drive three-phase induction motor". International Journal of Electrical & Computer Engineering (2088-8708) (2021) vol.11 (4) pp 1-9.

[19] Ayala, Magno, Jesus Doval-Gandoy, Osvaldo Gonzalez, Jorge Rodas, Raul Gregor, and Marco Rivera. "Experimental stability study of modulated model predictive current controllers applied to six-phase induction motor drives." IEEE Transactions on Power Electronics 36, no. 11 (2021): 13275-13284.

[20] Bhowate, Apekshit, Mohan V. Aware, and Sohit Sharma. "Predictive Torque Control of Five-Phase Induction Motor Drive Using Successive Cost Functions for CMV Elimination." IEEE Transactions on Power Electronics 36, no. 12 (2021): 14133-14141.

[21] Shawier, Abdullah, Abdelrahman Habib, Mohamed Mamdouh, Ayman Samy Abdel-Khalik, and Khaled H. Ahmed. "Assessment of predictive current control of six-phase induction motor with different winding configurations." IEEE Access 9 (2021): 81125-81138.

[22] Fereidooni, Arash, S. Alireza Davari, Cristian Garcia, and Jose Rodriguez. "Simplified Predictive Stator Current Phase Angle Control of Induction Motor with a Reference Manipulation Technique." IEEE Access 9 (2021): 54173-54183.

[23] Bassi, Hussain, Muhyaddin Jamal Hosin Rawa, M. Abbas Abbasi, Abdul Rashid Husain, Nik Rumzi Nik Idris, and Waqas Anjum. "Predictive flux control for induction motor drives with modified disturbance observer for improved transient response." U.S. Patent 11,031,891, issued June 8, 2021.

[24] Zhang, Yongchang, Xing Wang, Haitao Yang, Boyue Zhang, and Jose Rodriguez. "Robust predictive current control of induction motors based on linear extended state observer." Chinese Journal of Electrical Engineering 7, no. 1 (2021): 94-105.

[25] Mousavi, Mahdi S., S. Alireza Davari, Vahab Nekoukar, Cristian Garcia, and Jose Rodriguez. "Integral Sliding Mode Observer-Based Ultra-Local Model for Finite-Set Model Predictive Current Control of Induction Motor." IEEE Journal of Emerging and Selected Topics in Power Electronics (2021).

[26] Kiani, Babak. "A computationally low burden MPTC of induction machine without prediction loop and weighting factor." Bulletin of the Polish Academy of Sciences: Technical Sciences (2022): e142050-e142050

[27] Rodriguez, Jose, Cristian Garcia, Andres Mora, Freddy Flores-Bahamonde, Pablo Acuna, Mateja Novak, Yongchang Zhang et al. "Latest Advances of Model

Predictive Control in Electrical Drives—Part I: Basic Concepts and Advanced Strategies." IEEE Transactions on Power Electronics 37, no. 4 (2021): 3927-3942.

[28] Rodriguez, Jose, Cristian Garcia, Andres Mora, S. Alireza Davari, Jorge Rodas, Diego Fernando Valencia, Mahmoud Elmorshedy et al. "Latest advances of model predictive control in electrical drives—Part II: Applications and benchmarking with classical control methods." IEEE Transactions on Power Electronics 37, no. 5 (2021): 5047-5061.

[29] Mousavi, Mahdi S., S. Alireza Davari, Vahab Nekoukar, Cristian Garcia, and Jose Rodriguez. "Finite-Set Model Predictive Current Control of Induction Motors by Direct Use of Total Disturbance." IEEE Access 9 (2021): 107779-107790.

[30] Mamdouh, Mohamed, Ayman Samy Abdel-Khalik, and Mohamed A. Abido. "Predictive current control of asymmetrical six-phase induction motor without weighting factors." Alexandria Engineering Journal 61, no. 5 (2022): 3793-3803.

[31] Habib, Abdelrahman, Abdullah Shawier, M. Mamdouh, Ayman Samy Abdel-Khalik, Mostafa S. Hamad, and Shehab Ahmed. "Predictive current control based pseudo six-phase induction motor drive." Alexandria Engineering Journal 61, no. 5 (2022): 3937-3948

[32] Yang, Anxin, and Ziguang Lu. "Electromagnetic torque and reactive torque control of induction motor drives to improve vehicle variable flux operation and torque response." Journal of Power Electronics 22, no. 10 (2022): 1699-1712.

[33] Sharma, Sudhir, Bhoopendra Singh, and Ashutosh Datar. "Duty ratio control technique with torque ripple minimization for induction motor-based electric vehicle applications." Journal of Power Electronics 23, no. 4 (2023): 617-624.

[34] Qiu, Hongbo, Kun He, and Ran Yi. "Influence and optimization of split-winding on induction motor performance." Journal of Power Electronics (2023): 1-9.

[35] F. Yahiaoui, M. Boudour, and M. Tadjine, "Nonlinear control of induction motor using genetic algorithm optimization," in Proc. 2011 7th International Workshop on Systems, Signal Processing and their Applications, pp. 179-184.

[36] R. Venayagamoorthy, "Application of computational intelligence techniques for control of a small squirrel cage induction motor," in Proc. 2003 IEEE Swarm Intelligence Symposium, pp. 56-63.

[37] Mehedi, Ibrahim Mustafa, Nordin Saad, Muawia Abdelkafi Magzoub, Ubaid M. Al-Saggaf, and Ahmad H. Milyani. "Simulation analysis and experimental evaluation of improved field-oriented controlled induction motors incorporating intelligent controllers." IEEE Access 10 (2022): 18380-18394.

[38] T. Jalil, M. Boudour, and M. Tadjine, "Optimal tuning of induction motor control using gravitational search algorithm," in Proc. 2013 3rd International Conference on Systems and Control, pp. 208-213.

[39] J. Senthil Kumar, S. Himavathi, and A. Muthuramalingam, "Hybridization of gravitational search algorithm for multi-objective optimal power flow problem," in Proc. 2012 International Conference on Emerging Trends in Electrical Engineering and Energy Management, pp. 130-135.

[40] P. A. Naidu and V. Singh, "Speed control of induction motor and control of multilevel inverter output with optimal PI controller using DE and GSA optimization technique," 2018 3rd International Conference on Communication and Electronics Systems (ICCES), Coimbatore, India, 2018, pp. 920-927, doi: 10.1109/CESYS.2018.8724072.

[41] Chirantan, Shaswat, and Bibhuti Bhusan Pati. "Dynamics assessment of an inverter fed induction motor drive by an improved predictive controller leveraging finite control set mechanism." ITEGAM-JETIA 10, no. 47 (2024): 83-94.

[42] Chirantan, Shaswat, and Bibhuti Bhusan Pati. "Torque and dq axis current dynamics of an inverter fed induction motor drive that leverages computational intelligent techniques." AIMS Electronics and Electrical Engineering 8, no. 1 (2024): 28-52.

[43] Chirantan, Shaswat, and Bibhuti Bhusan Pati. "Integration of predictive and computational intelligent techniques: A hybrid optimization mechanism for PMSM dynamics reinforcement." AIMS Electronics and Electrical Engineering 8, no. 2 (2024): 255-281.